Age-Related Macular Degeneration Choroidal Vascular Distribution Characteristics Based on Indocyanine Green Angiography

Ke Wu,[1] Jiayi Wu,[1] Jing Yao,[1] Rundong Song,[2] Ruihua Jing,[1] Wenpeng Li,[1] Xuan Wang,[3] Nianjia Wang,[1] Yuping Zheng,[1] and Liang Yao[1]

[1]The Second Affiliated Hospital of Xi'an Jiaotong University, Xi'an, Shaanxi, China
[2]The First Affiliated Hospital of Xi'an Jiaotong University, Xi'an, Shaanxi, China
[3]Sound Physicians, 1800 N California St., Stockton, California, United States

Correspondence: Yuping Zheng and Liang Yao, The Second Affiliated Hospital of Xi'an Jiaotong University, No. 157 Xiwu Road, Xi'an, Shaanxi 710004, China;
zheng-tei@163.com and lyao0815@163.com.

KW and JW contributed equally to the work presented here and should therefore be regarded as equivalent authors.
YZ and LY contributed equally to this work.

Received: September 19, 2023
Accepted: December 15, 2023
Published: January 5, 2024

Citation: Wu K, Wu J, Yao J, et al. Age-related macular degeneration choroidal vascular distribution characteristics based on indocyanine green angiography. *Invest Ophthalmol Vis Sci.* 2024;65(1):16. https://doi.org/10.1167/iovs.65.1.16

Purpose. The purpose of this study was to present our findings of the distribution pattern of choroidal arteries and large veins in patients with age-related macular degeneration (AMD) using indocyanine green angiography (ICGA).

Methods. A retrospective analysis was conducted on 980 patients who underwent ICGA at The Second Affiliated Hospital of Xi'an Jiaotong University from 2017 to 2023, including 240 patients with AMD. Secondary image processing was applied to the angiographic videos to obtain posterior distribution maps of choroidal arteries and large veins. Differences between different distribution patterns regarding age, gender, eye laterality, and circulation time were compared. We also conducted a comparison of choroidal vascular distribution characteristics between patients with AMD and patients with diabetic retinopathy (DR) and provided a summary of choroidal vascular distribution patterns in AMD.

Results. The filling patterns of choroidal arteries can be classified into the invisible trunk arteries type, the partially masked trunk arteries type, and the exposed trunk arteries type. The vascular topography of the large choroidal vein can be classified into the watershed type, the non-watershed type, and the unknown type, further divided into six subtypes. The distribution patterns of choroidal arteries and veins were significantly correlated with age ($P < 0.001$). Left eye, older age, and the exposed trunk arteries type were independent risk factors for non-watershed large choroidal vein ($P < 0.05$). The non-watershed type was the main characteristic of the venous phase in AMD.

Conclusions. The distribution characteristics of the arterial and venous patterns in AMD suggest atrophy of the small blood vessels in the choroid and insufficient perfusion pressure of the blood flow.

Keywords: choroid, indocyanine green angiography (ICGA), vascular distribution pattern, age-related macular degeneration (AMD)

The choroid supplies the outer layer of the retina and stands as the most vascular tissue in the eyes, playing a crucial role in the anatomy, physiological metabolism, photoprotection, and immunity of the human eyes. Understanding the circulation patterns of the choroidal vessels is vital for comprehending diseases of the retina and choroid. Age-related macular degeneration (AMD), one of the most common vision-impairing diseases in ophthalmology, affects millions of people worldwide and stands as the leading cause of irreversible vision loss. There are two main types of AMD, neovascular AMD and non-neovascular AMD, which can be further classified based on specific features of the disease.[1] The pathogenesis of AMD remains unclear, and although treatment options, such as photodynamic therapy, antioxidant therapy, and anti-VEGF therapy exist, their effects are not fully satisfactory.[2,3] Therefore, exploring the mechanism of AMD is of great clinical significance.

Indocyanine green angiography (ICGA) was introduced to clinical ophthalmology in 1969. Leveraging its unique fluorescence properties, it is used to observe choroidal vessels in real-time, serving as an important tool for understanding the choroid.[4] In pioneering studies during the early 1970s, Hayreh et al. utilized ICGA to uncover the segmental distribution of choroidal vessels and the lobar arrangement pattern of choroidal capillaries. They demonstrated that the supply area of the short posterior ciliary artery is triangular in shape, with each unit independent of the others, by observing the in vivo circulation of the choroidal vascular bed beneath the macula.[5–10] The flaw of this pattern is that if the clinical significance of this vascular distribution characteristic is its susceptibility to the effects of ischemia when perfusion pressure in the vascular bed decreases. Choroidal neovascularization beneath the macula in AMD may be a response to chronic ischemia.[10] Based on experimental

vortex vein occlusion, Hayreh et al. identified a watershed zone of choroidal vortex veins, a cross-shaped area of low fluorescence that extends horizontally across the optic disc and the fovea and vertically across the optic disc region.[8] The venous tributaries from this watershed zone gradually drain into the vortex vein at the equator, and this drainage pattern, which aligns with the supply of the short posterior ciliary arteries, is essential for maintaining a high oxygen concentration in the outer retina. Thus, the existence of the watershed of the vortex veins is considered of significant importance by most researchers. Current scholarly work has focused on the symmetry of choroidal vasculature. For instance, Mori et al. used montage ICGA to evaluate 36 healthy eyes and found that 18 (50%) of them had an asymmetrical choroidal venous pattern, consistent with a preferential choroidal drainage pathway in the macula.[11] Hiroe and Kishi utilized swept source optical coherence tomography (SS-OCT) to examine the choroidal large vessel pattern in healthy eyes and those with central serous chorioretinopathy (CSC), discovering that 24 out of 39 eyes (62%) exhibited a symmetric distribution of choroidal large vessels.[12] Savastano et al. evaluated 154 healthy eyes from 77 patients, using a 3 mm × 3 mm en face OCT to observe and document various choroidal vascular patterns in the posterior pole.[13] Although these studies have concentrated on the choroidal large vessels, most are based on the en face mode of OCT, which, due to technical limitations[14] cannot display the blood circulation in the choroid or differentiate between arterial and venous vessels.

In this article, we capitalized on the real-time dynamic visualization capability of ICGA to scrutinize the angiography videos of a substantial population (980 cases). We observed the blood circulation of the choroid and innovatively classified the filling patterns of choroidal arteries. Further, we subdivided the topography of choroidal veins. Based on these findings, we summarized the vascular distribution patterns in patients with AMD and hypothesized about potential pathogenic mechanisms.

Materials and Methods

Participants

We performed a retrospective analysis of dynamic video recordings from 1297 patients who underwent ICGA examination in the ophthalmology outpatient and inpatient departments of The Second Affiliated Hospital of Xi'an Jiaotong University between September 2017 and February 2023. Collecting patient's name, gender, age, eye laterality, diagnosis, fundus photography (Canon Digital Retinal Camera CR-2 AF), and OCT images (GmbH 69121; Heidelberg Engineering, Heidelberg, Germany). The exclusion criteria included: (1) a history of severe systemic disease other than diabetes, such as uncontrolled hypertension, serious cardiovascular and cerebrovascular diseases, malignant tumors, etc.; (2) inability to maintain fixation due to eye tremor; (3) poor video quality due to corneal ulcer, moderate to severe cataract, etc.; and (4) a history of eye treatment, such as previous retinal laser photocoagulation or intraocular injection history. Finally, the study encompassed 980 eyes of 980 patients, including 240 eyes of 240 patients with AMD.

ICGA Operation Method

ICGA was conducted simultaneously with fluorescein fundus angiography (FFA) using a confocal laser synchronized angiography system (GmbH 69121; Heidelberg Engineering, Heidelberg, Germany). After verifying negative results for intradermal allergy testing with fluorescein sodium and indocyanine green, a mixture of 25 mg indocyanine green and 3 mL of 20% (10–20 mg/kg) fluorescein sodium in 2 mL of saline was completely dissolved and rapidly injected into the patient's elbow vein over a span of 5 seconds. After the injection, a 1-minute dynamic video recording of the fundus was performed, along with high-resolution, rapidly acquired 55 degrees digital images (992 × 596 pixel images, 5 frames per second). All angiograms were obtained by the same operator.

Image Selection

One arterial phase and one venous phase image were selected from each patient's ICGA angiography video, and the time of the selected images was recorded. The arterial phase refers to the moment when the choroidal arteries complete filling, while the veins have not yet been visualized (A time); the venous phase refers to the moment when the major veins are fully filled (V time). The time required for major vein filling (A-V time) is calculated by subtracting the two phases. It is worth noting that the selection of arterial and venous phase images for each patient in this study was jointly determined by a researcher, a senior fundus angiography technician, and an expert in fundus diseases. For examples of image selection, please refer to Supplementary Figure S1.

Image Processing

Image processing encompassed two main parts. The initial part involved processing selected ICGA arterial phase and venous phase images to extract the choroidal artery and large vein vessels. This extraction was performed via the threshold method using Fiji (available from https://imagej.net/Fiji/Downloads). For detailed instructions, please refer to Supplementary Figure S2.

The latter part of the process was concerned with the construction of 3D vascular models of the choroid. OCT Angiography (VG200i; SVision Imaging, Luoyang, China) was carried out on patients exhibiting three representative arterial filling patterns. For further vessel segmentation, two image processing software, Fiji and 3D Slicer (available from https://download.slicer.org), were utilized. Stacks displaying color were automatically segmented using the conventional machine learning image processing plugin, Trainable Weka Segmentation, to capture blood flow signals from the medium to large vessels in the choroid. These stacks were then imported into the 3D Slicer software. Initially, they were segmented automatically based on grayscale thresholding, followed by manual segmentation of the choroidal arteries and veins, guided by the entrance of the short posterior ciliary arteries, vessel alignment, morphological characteristics, and ICGA images.

Statistical Analysis

Quantitative data with a normal distribution was presented as the mean ± standard deviation and analyzed using an independent sample *t*-test or 1-way ANOVA, with the least significant difference (LSD) analysis used for multiple comparisons. Quantitative data not following a normal distribution were presented as median (interquartile range), with non-parametric tests used for analysis. Count data were

Investigative Ophthalmology & Visual Science

presented as the number of cases (percentage), and the chi-square test was applied for multiple group comparisons. Differences between groups were assessed using adjusted residual values. Univariate binary logistic regression analysis was conducted on the included independent variables, and variables with a P value of < 0.1 were integrated into the multivariate regression analysis.[15] The consistency test used the Kappa coefficient test. All statistical data were analyzed using SPSS 26.0 (SPSS, Inc., Chicago, IL, USA), and propensity score matching was performed using the Matchlt package in R version 4.2.1 (R Foundation for Statistical Computing, Vienna, Austria; http://www.r-project.org). A P value less than 0.05 was considered statistically significant.

Results

Arterial and Venous Vascular Distribution Patterns

The distribution patterns of choroidal arteries are categorized into three types (Figs. 1, 2, Supplementary Figs. S3–S5): invisible trunk arteries, partially masked trunk arteries, and exposed trunk arteries. The invisible trunk arteries pattern (see Figs. 1A1, 1A2) is characterized by a diffuse indistinct haze in the filling of the macular arteries (indicated by a white star), without evident vascular morphology in the posterior region. The partially masked trunk arteries pattern (see Figs. 1B1, 1B2) also exhibits a diffuse indistinct haze in the macular area (white star), but evident vascular morphology can be seen in the posterior region (white arrow). The exposed trunk arteries pattern (see Figs. 1C1, 1C2) is characterized by a nearly absent diffuse indistinct haze in the macular area, with visible vascular in the posterior region (white arrows).

The topographic patterns of the posterior major veins can be classified into six types (see Fig. 1): upper and lower straight, upper and lower curved, unknown, upper thick, lower thick, and intermediate anastomosis. The first two types are commonly referred to as watershed present types, whereas the latter three types are collectively known as watershed non-present types (the horizontal watershed across the optic disc and macula is indicated by the yellow dashed line in the Fig. 1). The upper and lower straight type (see Figs. 1D1, 1D2) refers to the major veins arranged in a straight line (white arrows), divided by a horizontal watershed. The upper and lower curved type (see Figs. 1E1, 1E2) is characterized by the major veins being curved above and below the horizontal watershed (white arrows). The unknown pattern (see Figs. 1F1, 1F2) shows lesions or abundant fluorescence of small and medium-sized blood vessels in the macular region, obscuring the true distribution of the major veins (white circular dashed line). The upper thick type (see Figs. 1G1, 1G2) is characterized by an increased diameter of the major veins above the horizontal watershed, extending downward (white arrow). Conversely, the lower thick type (see Figs. 1H1, 1H2) is characterized by an increased diameter of the major veins below the horizontal watershed, extending upward (white arrow). The intermediate anastomosis type (see Figs. 1I1, 1I2) refers to the convergence of the upper and lower major veins crossing the horizontal watershed in the macular region (white arrows).

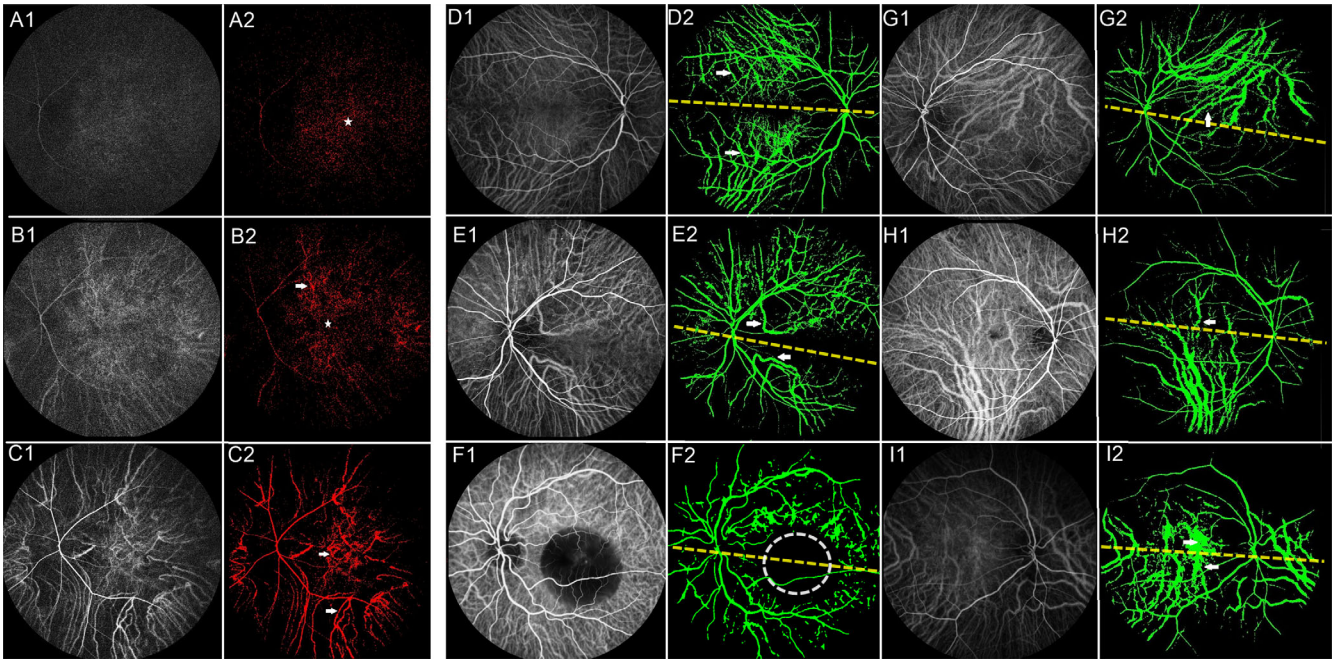

Figure 1. Distribution patterns of choroid arterial and major venous vessels (*red* indicates arterial pattern and *green* indicates venous pattern). A1 and A2 shows invisible trunk arteries pattern, B1 and B2 shows partially masked trunk arteries pattern, C1 and C2 shows exposed trunk arteries pattern, D1 and D2 shows upper and lower straight pattern, E1 and E2 shows upper and lower curved pattern, F1 and F2 shows unknown pattern, G1 and G2 shows upper thick pattern, H1 and H2 shows lower thick pattern, and I1 and I2 shows intermediate anastomosis pattern. In figures A1 to C2, the *white stars* indicate diffuse indistinct haze and the *white arrows* indicate evident vascular. In figures D1 to I2, the *yellow dashed line* represents the horizontal watershed across the optic disc and macula, the *white arrows* point out the vascular morphology, and the *white circle dotted line* represents the unknown distribution.

Investigative Ophthalmology & Visual Science

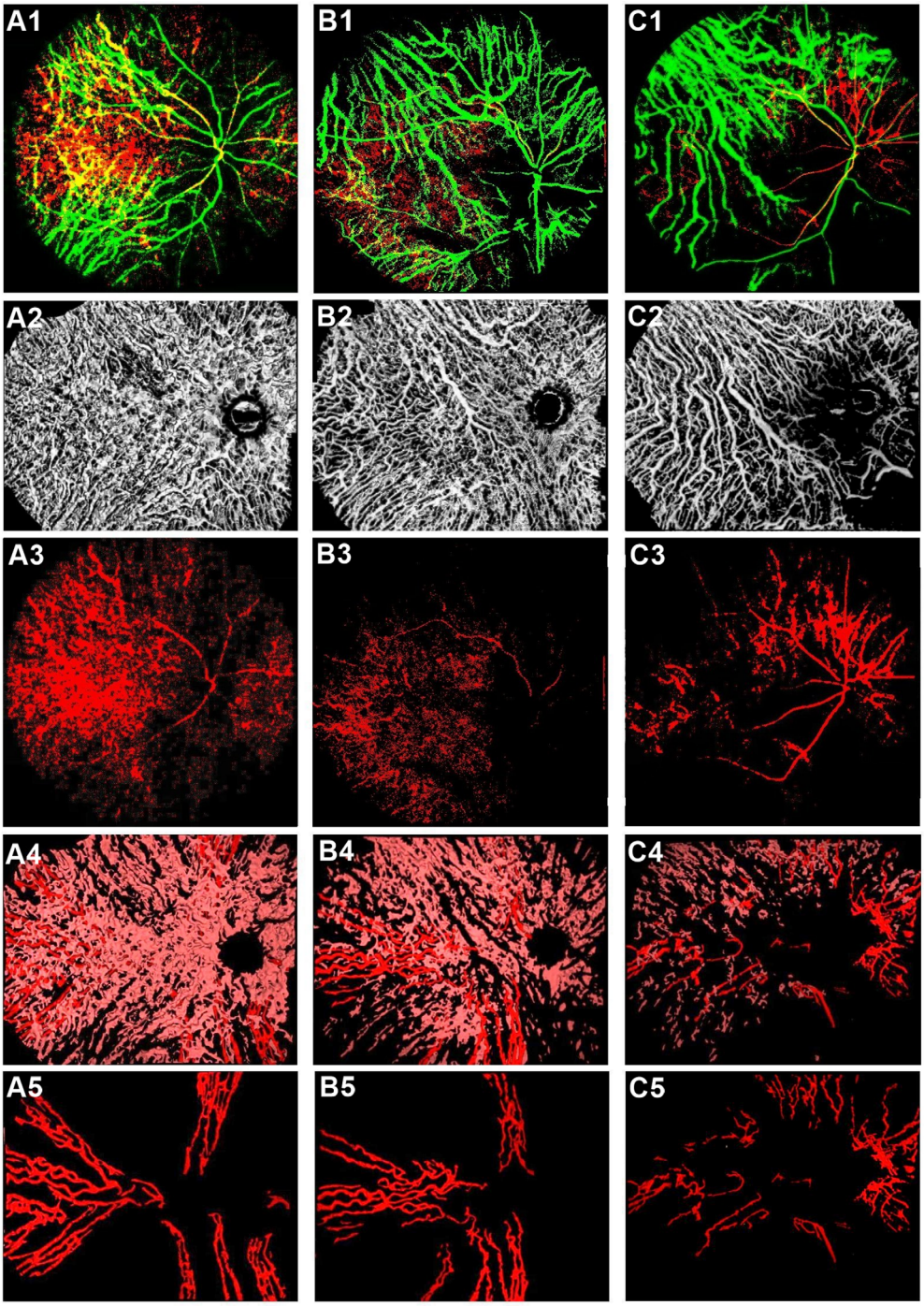

Figure 2. Three typical patients with arterial patterns. A1 to A5 showed an invisible trunk arteries pattern in a 35-year-old female patient with no significant abnormalities in ICGA. B1 to B5 showed a partially masked trunk arteries pattern in a 51-year-old female patient with a diagnosis of perivenous inflammation. C1 to C5 showed an exposed trunk arteries pattern in an 84-year-old male patient with a diagnosis of AMD. Shown from the *top* to *bottom* are the superimposed images of the arterial and venous phases after Fiji processing (A1, B1, C1), the structural images of the choroidal vessels displayed by OCTA (A2, B2, C2), the images of the arterial phase after Fiji processing (A3, B3, C3), the choroidal trunk arteries (*red* part) and middle vessel (*pink* part) models obtained by 3D slicer segmentation (A4, B4, C4), and the choroidal trunk arteries model obtained by the 3D slicer (A5, B5, C5).

Two researchers independently classified the patterns of choroidal arteries and veins in the included 980 patients (980 eyes) based on the processed images from the arterial and venous phases in Fiji. Disagreements were resolved by a senior expert in fundus diseases. The results showed a high consistency in the classification of arterial and venous vascular patterns by the two researchers ($P < 0.001$, Kappa coefficients of 0.799 and 0.739, respectively; see Supplementary Tables S1, S2).

Table 1. Basic Information Analysis of the Three Arterial Filling Patterns

	Invisible Trunk Arteries	Partially Masked Trunk Arteries	Exposed Trunk Arteries	*P* Value
Number	236	585	159	—
Gender (male/female)*	153/83	390/195	79/80	<0.001
Eye laterality (left/right)	111/125	291/294	84/75	0.524
Age (mean ± SD)*	52.22 ± 12.83	58.58 ± 11.56	65.32 ± 11.56	<0.001
A time (mean ± SD)	16.67 ± 3.01	16.52 ± 3.21	16.29 ± 2.97	0.487
V time (mean ± SD)*	30.91 ± 3.67	30.46 ± 4.44	29.24 ± 3.64	<0.001
A-V time (mean ± SD)*	14.23 ± 2.43	13.94 ± 3.02	12.95 ± 2.68	<0.001

SD, standard deviation.
* In the arterial pattern, there were between-group differences in gender (chi-square test), age (ANOVA), V time (ANOVA), and A-V time (ANOVA).

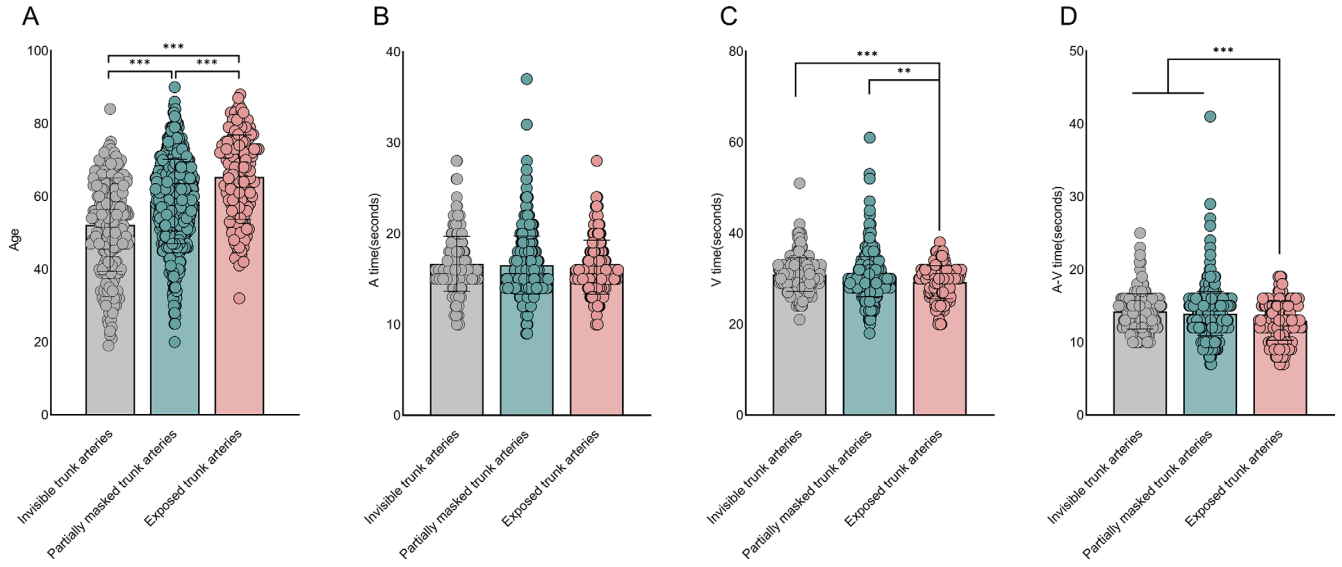

Figure 3. Scatter plots showing the differences in age (3A), A time (3B), V time (3C), and A-V time (3D) between the different arterial pattern groups, respectively. *$P < 0.05$, **$P < 0.01$, ***$P < 0.001$.

Basic Data Analysis of Arterial and Venous Vascular Pattern Classification

The comparison of ages among the three arterial filling patterns was statistically significant ($P < 0.001$; Table 1). The exposed trunk arteries pattern had a higher age compared to the partially masked trunk arteries pattern, and the partially masked trunk arteries pattern had a higher age compared to the invisible trunk arteries pattern (Fig. 3A). The average age for the invisible trunk arteries pattern was 52.22 ± 12.83 years, for the partially masked trunk arteries pattern was 58.58 ± 11.56 years, and for the exposed trunk arteries pattern was 65.32 ± 11.56 years. Female patients tended to have a preference for the exposed trunk arteries pattern, whereas male patients tended to have a preference for the partially masked trunk arteries pattern ($P < 0.001$; see Table 1). There was no statistically significant difference in A time among the three arterial filling patterns ($P = 0.487$; see Table 1), but there were statistically significant differences in V time and A-V time ($P < 0.001$; see Table 1). The exposed arterial pattern had an earlier V time compared to the other two patterns, and a shorter A-V time than the other two patterns (Figs. 3C, 3D)

The six types of large venous topographies did not significantly correlate with gender or eye laterality ($P = 0.596$ and $P = 0.066$; Table 2). Comparing the ages of the six venous topographies revealed a statistically significant difference ($P < 0.001$; see Table 2). The upper thick type and the lower thick type were associated with an older age group compared to the upper and lower straight type, as well as the unknown type (Fig. 4A). Additionally, the average age of the watershed non-existent type was significantly higher than that of the watershed existent type and the unknown type. The mean age of the watershed non-existent type was 60.52 ± 12.82, whereas the mean age of the watershed existent type was 56.28 ± 11.95 years ($P < 0.001$; as seen in Supplementary Table S3). The A time and A-V time of the six venous topographies were statistically significant ($P = 0.009$ and $P < 0.001$; see Table 2, Figs. 4B, 4D).

According to the cross-tabulation analysis (Supplementary Table S4) of the three arterial filling patterns and six major venous topographic maps, it can be observed that there is a statistically significant association between the two ($P < 0.001$). The intergroup differences were determined based on the adjusted standardized residuals, considering absolute values greater than 2 as significant. Therefore, it was found that the arterial filling pattern of invisible trunk arteries type is less likely to be associated with the upper thick veins, whereas the arterial filling pattern of the exposed trunk arteries type is less likely to be associated

Table 2. Basic Information Analysis of the Six Large Vein Topographic Maps

	Watershed Presence			Watershed Non-Presence			
	Upper and Lower Straight	Upper and Lower Curved	Unknown	Upper Thick	Lower Thick	Intermediate Anastomosis	*P* Value
Number	403	23	128	215	172	39	—
Gender (male/female)	262/141	13/10	84/44	135/80	110/62	20/19	0.596
Eye laterality (left/right)	181/222	12/11	72/56	120/95	85/87	16/23	0.066
Age, y* (M P25, P75)	56 (49, 64)	57 (45, 66)	57.5 (49, 64.75)	62 (52, 71)	63 (54, 69.75)	63 (46, 68)	<0.001
A time* (mean ± SD)	16.43 ± 2.93	15.61 ± 3.39	16.28 ± 3.10	16.52 ± 3.21	17.24 ± 3.44	15.64 ± 2.65	0.009
V time (M P25, P75)	30 (28, 32)	30 (29, 32)	31 (29, 33.75)	30 (28, 33)	30 (27, 33)	30 (29, 32)	0.377
A-V time* (M P25, P75)	14 (12, 15)	15 (14, 16)	15 (13, 16)	14 (12, 16)	13 (11, 15.75)	14 (13, 16)	<0.001

SD, standard deviation; M, median; P25, 25th percentile; P75, 75th percentile.
*In the venous pattern, there were between-group differences in age (Kruskal-Wallis rank sum test), A time (ANOVA), and A-V time (Kruskal-Wallis rank sum test).

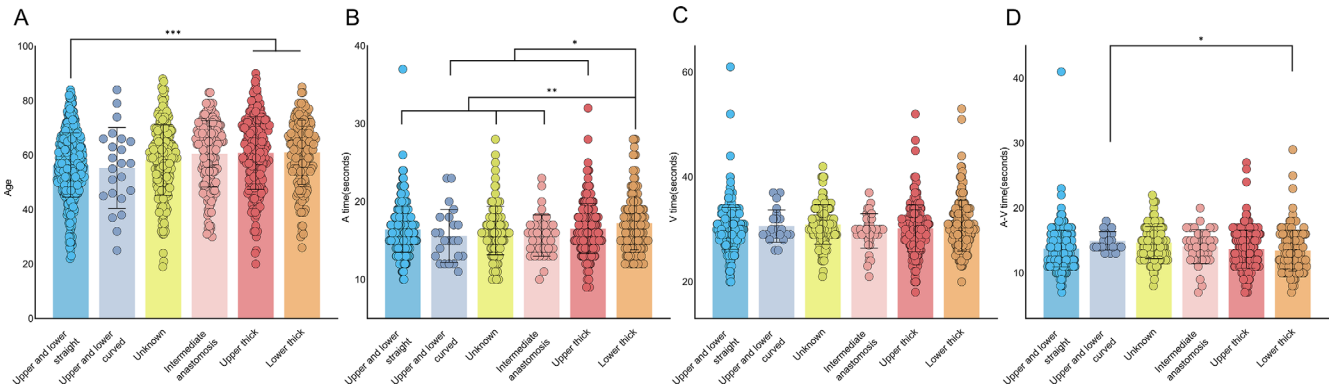

Figure 4. Scatter plots showing the differences in age (4A), A time (4B), V time (4C), and A-V time (4D) between the different venous pattern groups. *$P < 0.05$, **$P < 0.01$, ***$P < 0.001$.

with the upper and lower straight type major veins, but more likely to be associated with the upper thick veins.

Risk Factors for Non-Presence of Watershed in Large Veins

Univariate and multivariate binary logistic regression revealed that the left eye, older age, and the exposed trunk arteries filling pattern were independent risk factors for the absence of a significant venous watershed zone ($P < 0.05$; Table 3).

Characterization of Vascular Distribution Patterns in Patients With AMD

This study included a total of 980 patients (622 male patients, accounting for 63.47%; mean age of 58.14 ± 12.56 years; and 487 cases in the left eye, accounting for 49.69%). Among the 980 cases, 511 were diagnosed with diabetic retinopathy (DR) and 240 with AMD. The remaining cases included high myopia, retinal vein occlusion, anterior ischemic optic neuropathy, and ocular ischemia syndrome, among others. By matching with a 1:1 age-dependent propensity score, we included 178 patients with AMD and 178 patients with DR, and there were no differences in gender or eye laterality between the 2 in the matched cohort ($P > 0.05$; Table 4).

Comparing the arterial patterns between the two groups of patients, we found no obvious differences in the distribution of arterial patterns (Supplementary Fig. S6). Both groups were predominantly characterized by partially masked trunk arteries. However, there were substantial differences in the distribution of venous patterns between the two groups (Fig. 5A). Patients with DR were mainly classified as having a watershed pattern, particularly the upper and lower straight type, whereas patients with AMD were primarily classified as having a non-watershed pattern, especially the upper thick type. To further investigate the vascular distribution characteristics of the large veins in patients with AMD, we first divided the 240 patients with AMD into 2 types: neovascular AMD (189 cases) and non-neovascular AMD (51 cases). Comparing the venous distribution patterns between the two types, we found no significant differences (Fig. 5B). Both types were predominantly characterized by a non-watershed pattern. To further investigate the venous topography of both types of AMD in more detail, we performed a refinement of each of them. In the case of non-neovascular AMD, we categorized 51 patients into 3 stages according to Beckman's classification[16]: early (9 cases), intermediate (33 cases), and geographic atrophy (late stage, 9 cases). We found that the venous distribution of non-neovascular AMD was still dominated by the watershed absent type, especially the upper thick type, in which the proportion of upper and lower straight type in early AMD was higher than that of the other two types, and the proportion of watershed absent type was the highest in geographic atrophy (Fig. 5C). Among the neovascular AMD cases, we further subdivided them into three subtypes based on the

Table 3. Univariate and Multivariate Analysis of the Absence of Watershed in Large Veins

	Univariate Analysis OR (95% CI)	*P* Value	Multivariate Analysis OR (95% CI)	*P* Value
Female	1.129 (0.854~1.491)	0.394		
Left eye*	1.301 (0.9994~1.704)	0.055	1.330 (1.010~1.753)	0.043
Age, y*	1.028 (1.017~1.040)	<0.001	1.024 (1.012~1.036)	<0.001
A time	1.036 (0.992~1.082)	0.111		
V time	1.008 (0.976~1.040)	0.638		
A-V time	0.976 (0.931~1.022)	0.299		
Arterial patterns (Reference: Exposed trunk arteries*)				
Invisible trunk arteries	0.379 (0.243~0.591)	<0.001	0.518 (0.323~0.829)	0.006
Partially masked trunk arteries	0.496 (0.339~0.726)	<0.001	0.574 (0.389~0.849)	0.005

* Left eye, older age, and exposed trunk arteries filling pattern are independent risk factors for the absence of a horizontal watershed.

Table 4. Comparison of the Basic Data Between the Two Groups After Propensity Score Matching

	AMD	DR	*P* Value
Number	178	178	—
Gender (male/female)	118/60	104/74	0.126
Eye laterality (right/left)	86/92	82/96	0.671
Age, y	64.30 ± 0.60	64.25 ± 0.60	0.953

origin and location of the neovascularization.[17] By combining the fundus color photographs and OCT images of the included 189 cases of neovascular AMD, we ultimately classified them into type 1 macular neovascularization (MNV; 53 cases), type 2 MNV (135 cases), and type 3 MNV (1 case). Due to the limited number of type 3 MNV cases, we only compared the venous distribution patterns between type 1 MNV and type 2 MNV, and found no significant differences (Fig. 5D).

Discussion

The blood supply to the choroid may be the highest per unit tissue weight in the human body, surpassing that of the brain by 10 times. This robust blood flow helps to maintain a higher oxygen tension in the choroid than in the retina.[18] ICGA imaging delineates that the choroidal circulation can be segmented into three stages: early, middle, and late.[19] At present, there is no consensus on the precise timing of the choroidal circulation compared to the retinal

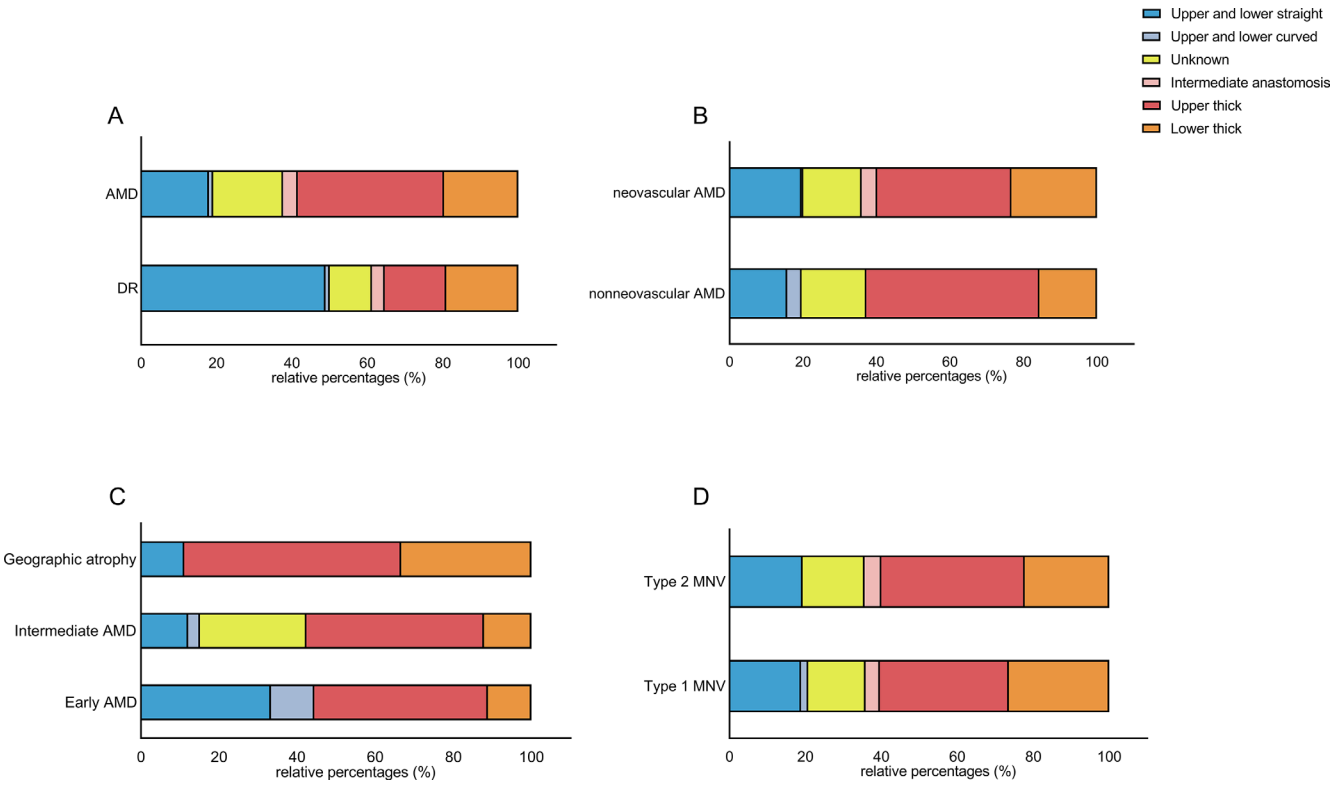

Figure 5. Showing stacked histograms comparing venous patterns in different subgroups, with a common legend for **A** to **D** in the upper right corner. (**A**) Comparison of venous distribution patterns between patients with AMD and patients with DR. (**B**) Comparison of venous distribution patterns between neovascular AMD and non-neovascular AMD. (**C**) Comparison of venous distribution patterns among early AMD, intermediate AMD, and geographic atrophy. (**D**) Comparison of venous distribution patterns between type 1 MNV and type 2 MNV.

circulation. By observing early imaging videos, we classified the choroidal arterial filling pattern into three types: the invisible trunk arteries, the partially masked trunk arteries, and the exposed trunk arteries. With age, we observed a gradual transition from the invisible trunk arteries to the exposed trunk arteries, accompanied by a shortening in venous filling time. Using the 3D slicer, we constructed 3D vascular models of the choroidal vessels from angiography of 3 patients exhibiting typical arterial filling patterns. As shown in Figure 2 and Supplementary Figures S3–S5, middle vessels atrophy and loss, gradually aggravation from the invisible trunk arteries to the partially masked trunk arteries then to the exposed trunk arteries, indicating reduced perfusion of the small vessels in the choroid, possibly leading to a shortened choroidal vascular substance exchange time.[20] Our study also discovered that women are more prone to display an exposed trunk arteries pattern of arterial filling, and previous studies have noted that choroidal thickness (CT) in women is thinner than that in men,[21,22] which might account for this phenomenon.

We categorized the large veins into three primary types: watershed, non-watershed, and unknown, with six subtypes. The age of the non-watershed type is greater than the watershed type, and patients with the exposed trunk arteries type often display the non-watershed large venous type, aligning with our research results. Some reports have also revealed that the left eye's CT and choroidal volume (CV) are thicker than the right eye's in all regions.[23] Our study indicates that non-watershed large veins are more likely to occur in the left eye, suggesting that the left eye's blood vessels might have a larger diameter and volume, making it easier to cross the horizontal watershed once venous congestion and dilation occur.

Research indicates that the CT of patients with DR is thinner compared to that of healthy individuals, with the thinning increasing significantly as DR progresses. This thinning is speculated to be tied to damage in the choriocapillaris.[24] Various studies have also discovered that the density of choroidal capillaries significantly decreases as DR advances.[25,26] Due to the current lack of evidence regarding the impact of DR on choroidal microvasculature, our working hypothesis is that the damage inflicted by DR primarily affects choroidal capillaries. As a result, for the purpose of studying choroidal microvasculature, we classified DR patients as the "control group." Upon examining Figure 2 (A4-C4), we observed that atrophy in choroidal arteries is most pronounced in the macular region. Previous studies have shown that, with increasing age, the fluorescence intensity of arterial filling in the macular area gradually weakens, and the number of arterial vessels progressively diminishes in ICGA of healthy individuals. This reduction in blood flow in the macular area is presumably related to the emergence of certain macular diseases, such as AMD.[27] Our 3D vascular models lend support to this hypothesis.

Several theories attempt to explain the pathogenesis of AMD, including primary retinal pigment epithelium (RPE) and Bruch's membrane aging, primary genetic defects, and primary abnormalities in ocular perfusion.[28] In patients with AMD, ICGA has identified the phenomenon of delayed arterial filling, indicating insufficient ocular perfusion.[29,30] These studies indicate from the aspect of contrast filling time that patients with AMD have insufficient perfusion of ocular blood flow. It is worth mentioning that our study provides evidence to support this viewpoint from the perspective of the distribution of choroidal vascular morphology. We found that the distribution pattern of large veins in patients with AMD differs from that in the control group. Previous studies on thick choroidal neovascularization lesions suggested a correlation between the dilation of choroidal outer layer vessels and chronic capillary ischemia. In our study, we found that as age increases, the atrophy of small layer arteries in the choroid increases. Compared to the control group, patients with AMD predominantly exhibit a pattern of large veins without watershed. Therefore, we speculate that the insufficient perfusion of choroidal arterial blood flow in patients with AMD results in poor venous reflux and stasis, leading to vessel dilation that surpasses the horizontal watershed. Due to the influence of gravity, venous reflux from above becomes more difficult. As a result, patients with AMD exhibit a higher proportion of thick and robust veins in the superior region.

Our study benefits from a relatively large sample size, with 980 patients undergoing angiography for analysis. Furthermore, we leveraged the real-time fluorescence characteristics of angiography to classify the vascular perfusion patterns of the choroidal arteries and to further categorize the choroidal venous topography. This approach has provided evidence suggesting that the pathogenesis of AMD is associated with inadequate choroidal perfusion. However, our study does have its limitations. We did not collect angiography data from healthy individuals. This omission limits our ability to reflect objectively the distribution patterns of arterial and venous vessels in a normal population. Meanwhile, this is a retrospective study, and hindered by the lack of detailed information, there are some thoughts that could not be confirmed, such as perhaps there is also a further relationship of vascular distribution pattern of patients with AMD with age at onset? This deserves to be verified in a next cohort study.

Acknowledgments

Supported by the National Natural Science Foundation of China (Nos. 82201163).

Disclosure: **K. Wu**, None; **J. Wu**, None; **J. Yao**, None; **R. Song**, None; **R. Jing**, None; **W. Li**, None; **X. Wang**, None; **N. Wang**, None; **Y. Zheng**, None; **L. Yao**, None

References

1. Thomas CJ, Mirza RG, Gill MK. Age-related macular degeneration. *Med Clin North Am*. 2021;105(3):473–491.
2. Nowak JZ. Age-related macular degeneration (AMD): pathogenesis and therapy. *Pharmacol Rep PR*. 2006;58(3):353–363.
3. Ruan Y, Jiang S, Gericke A. Age-related macular degeneration: role of oxidative stress and blood vessels. *Int J Mol Sci*. 2021;22(3):1296.
4. Yannuzzi LA, Ober MD, Slakter JS, et al. Ophthalmic fundus imaging: today and beyond. *Am J Ophthalmol*. 2004;137(3):511–524.
5. Hayreh SS. The choriocapillaris. *Albrecht Von Graefes Arch Klin Exp Ophthalmol*. 1974;192(3):165–179.
6. Hayreh SS. Segmental nature of the choroidal vasculature. *Br J Ophthalmol*. 1975;59(11):631–648.
7. Hayreh SS, Baines JA. Occlusion of the posterior ciliary artery. I. Effects on choroidal circulation. *Br J Ophthalmol*. 1972;56(10):719–735.
8. Hayreh SS, Baines JA. Occlusion of the vortex veins. An experimental study. *Br J Ophthalmol*. 1973;57(4):217–238.

9. Hayreh SS. Proceedings: anatomy and pathophysiology of ocular circulation. *Exp Eye Res*. 1973;17(4):387–388.
10. Hayreh SS. Submacular choroidal vascular pattern. Experimental fluorescein fundus angiographic studies. *Albrecht Von Graefes Arch Klin Exp Ophthalmol*. 1974;192(3):181–196.
11. Mori K, Gehlbach PL, Yoneya S, Shimizu K. Asymmetry of choroidal venous vascular patterns in the human eye. *Ophthalmology*. 2004;111(3):507–512.
12. Hiroe T, Kishi S. Dilatation of asymmetric vortex vein in central serous chorioretinopathy. *Ophthalmol Retina*. 2018;2(2):152–161.
13. Savastano MC, Rispoli M, Savastano A, Lumbroso B. En face optical coherence tomography for visualization of the choroid. *Ophthalmic Surg Lasers Imaging Retina*. 2015;46(5):561–565.
14. Spaide RF, Klancnik JM, Cooney MJ. Retinal vascular layers imaged by fluorescein angiography and optical coherence tomography angiography. *JAMA Ophthalmol*. 2015;133(1):45–50.
15. Won HJ, Sung KR, Shin JW, Jo YH, Song MK. Comparison of lamina cribrosa curvature in pseudoexfoliation and primary open-angle glaucoma. *Am J Ophthalmol*. 2021;223:1–8.
16. Ferris FL, Wilkinson CP, Bird A, et al. Clinical classification of age-related macular degeneration. *Ophthalmology*. 2013;120(4):844–851.
17. Spaide RF, Jaffe GJ, Sarraf D, et al. Consensus nomenclature for reporting neovascular age-related macular degeneration data: consensus on neovascular age-related macular degeneration nomenclature study group. *Ophthalmology*. 2020;127(5):616–636.
18. Nickla DL, Wallman J. The multifunctional choroid. *Prog Retin Eye Res*. 2010;29(2):144–168.
19. Dzurinko VL, Gurwood AS, Price JR. Intravenous and indocyanine green angiography. *Optom St Louis Mo*. 2004;75(12):743–755.
20. Rosenfeld PJ, Trivizki O, Gregori G, Wang RK. An update on the hemodynamic model of age-related macular degeneration. *Am J Ophthalmol*. 2022;235:291–299.
21. Gupta P, Jing T, Marziliano P, et al. Distribution and determinants of choroidal thickness and volume using automated segmentation software in a population-based study. *Am J Ophthalmol*. 2015;159(2):293–301.e3.
22. Ooto S, Hangai M, Yoshimura N. Effects of sex and age on the normal retinal and choroidal structures on optical coherence tomography. *Curr Eye Res*. 2015;40(2):213–225.
23. Orduna E, Sanchez-Cano A, Luesma MJ, Perez-Navarro I, Abecia E, Pinilla I. Interocular symmetry of choroidal thickness and volume in healthy eyes on optical coherence tomography. *Ophthalmic Res*. 2018;59(2):81–87.
24. Horváth H, Kovács I, Sándor GL, et al. Choroidal thickness changes in non-treated eyes of patients with diabetes: swept-source optical coherence tomography study. *Acta Diabetol*. 2018;55(9):927–934.
25. Yang D, Cao D, Huang Z, et al. Macular capillary perfusion in Chinese patients with diabetic retinopathy obtained with optical coherence tomography angiography. *Ophthalmic Surg Lasers Imaging Retina*. 2019;50(4):e88–e95.
26. Lupidi M, Cerquaglia A, Gujar R, et al. Functional correlation between choroidal and retinal vascularity in low-grade diabetic retinopathy. *Acta Diabetol*. 2020;57(8):983–990.
27. Ito YN, Mori K, Young-Duvall J, Yoneya S. Aging changes of the choroidal dye filling pattern in indocyanine green angiography of normal subjects. *Retina Phila Pa*. 2001;21(3):237–242.
28. Ciulla TA, Harris A, Martin BJ. Ocular perfusion and age-related macular degeneration. *Acta Ophthalmol Scand*. 2001;79(2):108–115.
29. Remulla JF, Gaudio AR, Miller S, Sandberg MA. Foveal electroretinograms and choroidal perfusion characteristics in fellow eyes of patients with unilateral neovascular age-related macular degeneration. *Br J Ophthalmol*. 1995;79(6):558–561.
30. Böker T, Fang T, Steinmetz R. Refractive error and choroidal perfusion characteristics in patients with choroidal neovascularization and age-related macular degeneration. *Ger J Ophthalmol*. 1993;2(1):10–13.

Investigative Ophthalmology & Visual Science